

Color Embedding and Recovery Using Wavelet Packet Transform with Pseudorandomized Saturation Code

Kyung-Woo Ko, Dae-Chul Kim, Wang-Jun Kyung and Yeong-Ho Ha[▲]

School of Electronics Engineering, Kyungpook National University, 1370 Sankyuk-dong, Buk-gu,
Daegu 702-701, Korea
E-mail: yha@ee.knu.ac.kr

Abstract. Color embedding and recovery are investigated using a wavelet transform that enables color information to be hidden in gray images and then retrieved to recover color images. In a wavelet transform, high-frequency subbands are replaced by chrominance information from an image, yet the use of subbands can cause some loss of details and saturation. Therefore, this article proposes color embedding and recovery using a wavelet packet transform with a pseudorandom code to embed saturation information. In the color-to-gray process, the RGB is first converted to YCbCr color space to perform a two-level wavelet packet transform for a Y image. The CbCr color components are then embedded into the two subbands with the minimum amount of energy in the Y image, thereby minimizing the loss of details when compared to using a wavelet transform. In addition, to compensate the color saturation, the maximum and minimum values of the CbCr components from the original image are embedded into the diagonal-diagonal subband in a pseudorandom code form. In the recovery process, the saturation of the recovered image is compensated by applying the ratio of the original CbCr values to the extracted CbCr values. Experimental results show that the proposed method improves the color saturation of the recovered image when comparing the color difference and peak signal-to-noise values. © 2011 Society for Imaging Science and Technology.
[DOI: 10.2352/J.ImagingSci.Technol.2011.55.3.030501]

INTRODUCTION

Gray to color, known as colorization, is the process of adding color to monochrome images, such as old black-and-white photos, classic movies, and scientific illustrations. Colorization algorithms generally involve color mapping according to a colormap that has been determined by human assessment.^{1,2} Alternatively, reference images have recently been used to recover the color of gray images.^{3–11}

Thus, colorization algorithms can be divided into two categories. In the first category, arbitrary colors are added to monochrome images according to determined areas, regardless of the colors of the original images.^{1,2} For example, pseudocoloring colorizes an image based on its grayscale values mapped to a full RGB color range. Thus, pseudocolor images can help to reveal image qualities that would not be readily visible with a true color image.

Meanwhile, in the second category, the colors are recov-

ered using reference images with similar characteristics. For example, the original colors are restored based on the luminance distribution between a monochrome target image and a reference color image.^{3–5} Here, the target image is transformed into the luminance channel, while the reference image is transformed into the luminance and chromatic channels. The luminance distribution between the monochrome target and reference color images is then compared, and the chromatic information for the best matching region in the reference image is transferred to the target region. Consequently, the monochrome target image is colorized using the colors from the reference image, allowing the recovered colors of the target image to approximate the original image. However, since this type of method uses reference images, the colors of the target image are not exactly recovered.

Therefore, to recover colors that are similar to those of the original image, various algorithms using wavelet transform have been proposed.^{6–8} The main idea of this method is that the process of embedding and extracting color information is implemented using a wavelet transform. The color information which is CbCr of YCbCr color space or in-phase and quadrature (IQ) of YIQ color space is embedded into the vertical, horizontal, and diagonal subbands of the wavelet-transformed Y image, and a new gray image is obtained using an inverse wavelet transform. The color image is converted into a grayscale image, printed on a black-and-white printer. After the user scans the printed image, the decoder can then recover the colors using the wavelet transform. However, contour details are lost to some extent in the recovered color image, as the algorithm uses the high-pass vertical, horizontal, and diagonal subbands to embed the color information. Also, the color saturation is somewhat decreased as the pixel values for the new gray image are changed by the printing and scanning process.

To improve the above-mentioned deterioration, we previously proposed an embedding and recovery method based on a wavelet packet transform (WPT).⁹ In this method, a wavelet packet transform is applied to divide the Y image into 16 subbands and the total energy analyzed for each subband. The CbCr images are then embedded into two subbands. In addition, the color saturation of the recovered color image is improved by using the characteristic curve obtained between the printer and the scanner, thereby compensating for the change of pixel values between the printing

[▲]IS&T Member.

Received Jul. 30, 2010; accepted for publication Mar. 5, 2011; published online Apr. 11, 2011.

1062-3701/2011/55(3)/030501/10/\$20.00.

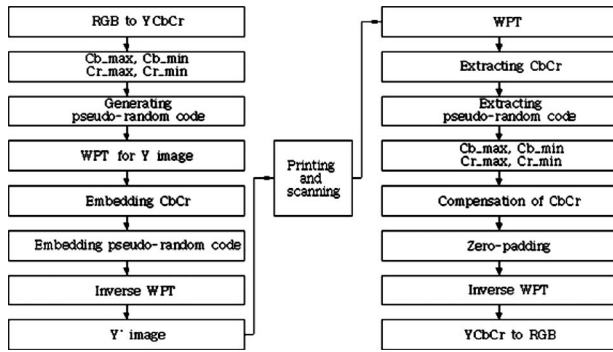


Figure 1. Flowchart of the proposed colorization method.

and scanning process. However, since the characteristic curve is invariably automatically changed when changing the printer and scanner model, this saturation compensating method is difficult to apply to most printer and scanner models.

Accordingly, this article proposes color embedding and recovery using a pseudorandomized saturation code based on a wavelet packet transform to improve the color saturation of the recovered color image and preserve as many details as possible from the original image. In the color-to-gray process, the Y image is divided into 16 subbands using a two-level wavelet packet transform. To minimize the loss of detail, the CbCr color components are then embedded into the two subbands with the minimum amount of energy in the Y image, where the selected combination of subbands is determined by investigating various combinations of eight subbands. Furthermore, to compensate the color saturation, the CbCr components are scaled using the maximum and minimum values of the CbCr components from the original image. These values are embedded into the diagonal-diagonal (DD) subband and transformed into a pseudorandom code while considering the visibility in the resulting gray image. In other words, the pseudorandom code includes the maximum and minimum values of the CbCr components in the original image and is expressed using numbers of white pixels. However, to reduce the degradation of details when using the pseudorandom code in the wavelet packet transform, the number of pixels is down sampled in the diagonal-diagonal subband. Finally, the ratio of the original CbCr values to the extracted CbCr values is applied to enhance the saturation of the recovered color image.

COLOR EMBEDDING AND RECOVERY USING AN EMBEDDED PSEUDORANDOM CODE

This article proposes color embedding and recovery using a pseudorandomized saturation code in a WPT, thereby reducing the degradation of saturation and preserving the details of the original image. Figure 1 shows a flowchart of the proposed colorization method. A two-level wavelet packet transform is used to embed the color information in a gray image.⁹ To minimize the loss of detail, two subbands are then selected for embedding the CbCr components. Next, to reduce the degradation of saturation, the maximum and minimum values of the CbCr components from the original

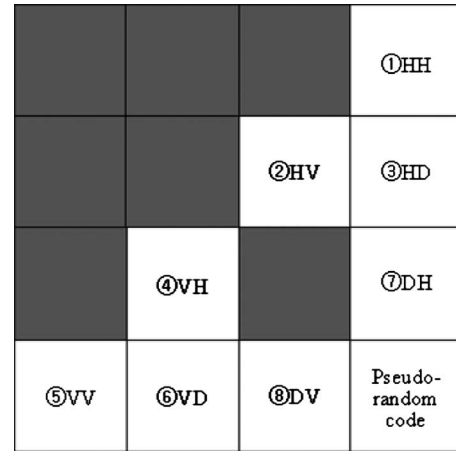


Figure 2. Subband locations for embedding the CbCr components.

image are embedded into the diagonal-diagonal subband using a pseudorandom code. After that, the method used to recover the colors from the new gray image with texture is the reverse process of the above color-to-gray algorithm.⁹

Subband Selection for Embedding CbCr

To minimize the loss of detail, a two-level wavelet packet transform is used to embed color information in a gray image, and two subbands are selected for embedding the CbCr components. Figure 2 shows the subband locations selected for embedding the CbCr components. Here, eight candidate subbands were selected: the horizontal-horizontal (HH), horizontal-vertical (HV), horizontal-diagonal (HD), vertical-horizontal (VH), vertical-vertical (VV), vertical-diagonal (VD), diagonal-horizontal (DH), and diagonal-vertical (DV) subbands. The seven subbands in the dark region in Fig. 2 were excluded, as they included relatively much more information on the original image than the other subbands. The DD subband was also excluded, as it was used to embed the pseudorandom code to compensate for the color saturation. Thus, the eight candidate subbands yielded 28 possible combinations of two subbands for embedding the CbCr components, and each combination was simulated. The results are shown in Table 1 and Figures 3 and 4, while the amount of energy for each combination is shown in Figure 5. The subbands used to embed the Cb and Cr components are selected based on their color difference in CIELAB color space and peak signal-to-noise (PSNR) values. As uniform changes of the components in $L^*a^*b^*$ color space correspond to uniform changes in the perceived color, the relative perceptual differences between any two colors in $L^*a^*b^*$ were approximated by treating each color as a point in three-dimensional space (with three components: L^* , a^* , and b^*) and measuring the Euclidean distance between them. Thus, the color differences in CIELAB color space and PSNR values were calculated as follows:

$$\Delta E_{ab}^* = (\Delta L^{*2} + \Delta a^{*2} + \Delta b^{*2})^{1/2} \quad (1)$$

where

$$\Delta L^* = L_2 - L_1, \quad \Delta a^* = a_2 - a_1, \quad \Delta b^* = b_2 - b_1.$$

Table I. Performance comparison of the recovered color images according to the location of the two subbands used to embed the CbCr components.

	Color difference			PSNR (dB)		
	Fruit	Balloon	Eagle	Fruit	Balloon	Eagle
1 and 2	5.93	5.14	4.06	27.42	27.17	30.39
1 and 3	6.01	5.20	4.09	27.24	27.08	30.22
1 and 4	5.95	5.15	4.05	27.32	27.20	30.41
1 and 5	6.52	5.34	4.28	25.47	26.74	29.41
1 and 6	6.04	5.17	4.11	27.07	27.14	30.16
1 and 7	5.91	5.18	4.03	27.43	27.18	30.44
1 and 8	5.92	5.16	4.06	27.45	27.18	30.36
2 and 3	5.82	4.71	3.98	27.65	27.71	30.87
2 and 4	5.73	4.67	3.93	27.90	27.86	31.12
2 and 5	6.33	4.87	4.17	25.76	27.35	29.95
2 and 6	5.87	4.69	3.99	27.47	27.80	30.82
2 and 7	5.79	4.66	3.92	27.75	27.87	31.14
2 and 8	5.75	4.64	3.94	27.82	27.88	31.05
3 and 4	5.88	4.92	3.97	27.58	27.72	30.92
3 and 5	6.42	5.14	4.20	25.65	27.20	29.81
3 and 6	5.97	4.95	4.03	27.29	27.65	30.64
3 and 7	5.85	4.97	3.96	27.68	27.64	30.95
3 and 8	5.84	4.88	3.98	27.69	27.73	30.87
4 and 5	6.39	4.91	4.16	25.66	27.33	29.98
4 and 6	5.94	4.72	3.97	27.30	27.77	30.83
4 and 7	5.80	4.68	3.91	27.75	27.89	31.17
4 and 8	5.79	4.66	3.93	27.77	27.89	31.08
5 and 6	6.42	4.91	4.20	25.51	27.28	29.75
5 and 7	6.33	4.85	4.14	25.77	27.38	30.00
5 and 8	6.33	4.84	4.17	25.77	27.37	29.93
6 and 7	5.85	4.88	3.97	27.51	27.77	30.87
6 and 8	5.89	4.93	3.99	27.46	27.70	30.79
7 and 8	5.76	4.68	3.92	27.90	27.89	31.11

$$\text{PSNR}_k = 20 \log_{10} \left(\frac{255}{\sqrt{\text{MSE}_k}} \right), \quad k = R, G, B \quad (2)$$

where

$$\text{MSE}_k = \frac{1}{mn} \sum_{i=0}^{m-1} \sum_{j=0}^{n-1} \|O_k(i,j) - R_k(i,j)\|^2.$$

here L_1 , a_1 , and b_1 are the CIELAB values of the original image, L_2 , a_2 , and b_2 are the CIELAB values of the recovered color image, (i, j) are the coordinates of an $m \times n$ image, k is the RGB color channels, and $O(i, j)$ and $R(i, j)$ denote the pixel values of the original image and recovered color image, respectively. If it is assumed that there is no loss of Y information during the process of embedding and extracting the

CbCr components, the ideal value of the color difference for each test image would be zero, and the experimental PSNR value for the fruit, balloon, and eagle images would be 29.80, 30.20, and 32.94, respectively.

Table I shows the HV-VH subbands resulted in the best performance for the fruit image, while the VH-DH subbands produced the best performance for the eagle image. However, for the balloon image, the HV-DV subbands delivered the best results as regard to the color difference, while the DH-DV subbands produced in the best performance as regard to the PSNR value. In other words, the combination of two subbands that resulted in the best performance as regard to the color difference and PSNR value depended on the image. Nonetheless, when analyzing all the figures in Table I, the best color difference and PSNR value were obtained

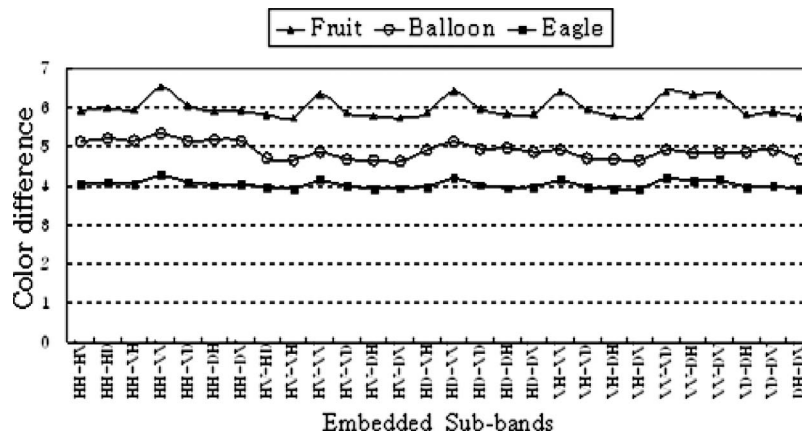


Figure 3. Color difference comparison of the recovered color images according to the location of the two subbands used to embed the CbCr components.

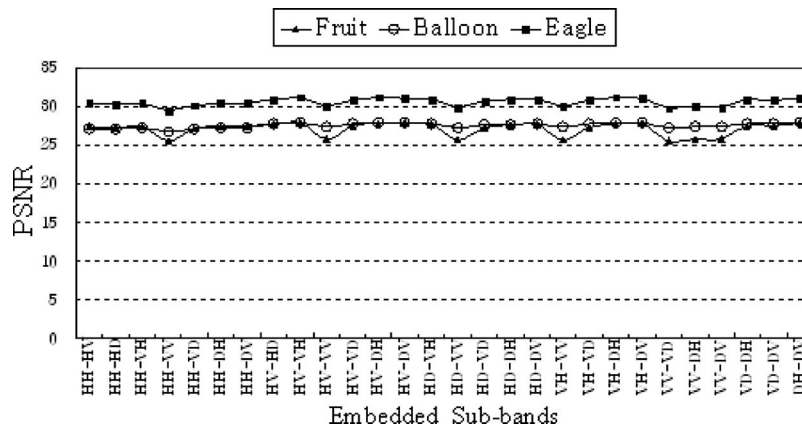


Figure 4. PSNR comparison of the recovered color images according to the location of the two subbands used to embed the CbCr components.

when using combinations among the HV, VH, DH, and DV subbands possibly because they included the minimum information on the original image, as mentioned in the previous section. The averaged color difference value when using combinations among the HV, VH, DH, and DV subbands was 4.79, whereas the averaged color difference value with combinations among the other subbands was 5.04. Similarly, the averaged PSNR value when using combinations among the HV, VH, DH, or DV subbands was 28.94, whereas the averaged PSNR value with combinations among the other subbands was 28.22.

Therefore, combinations of two subbands among the HV, VH, DH, and DV subbands produced the best recovered color image, except in the case of an extreme image, such as a checkered pattern. Consequently, in this study, the CbCr components were always embedded into the HV and VH subbands.

Notwithstanding, all eight subbands can conceivably be utilized to embed the CbCr components. In other words, to reduce the interpolation errors in the gray-to-color process, one-quarter of the CbCr images can be used instead of one-sixteenth of the individual CbCr images. A method of embedding one-quarter of the size CbCr components using all

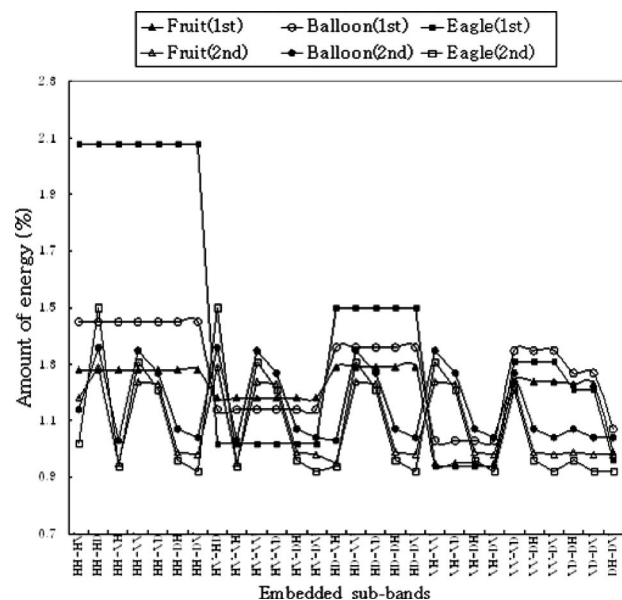


Figure 5. Amount of energy for each combination.

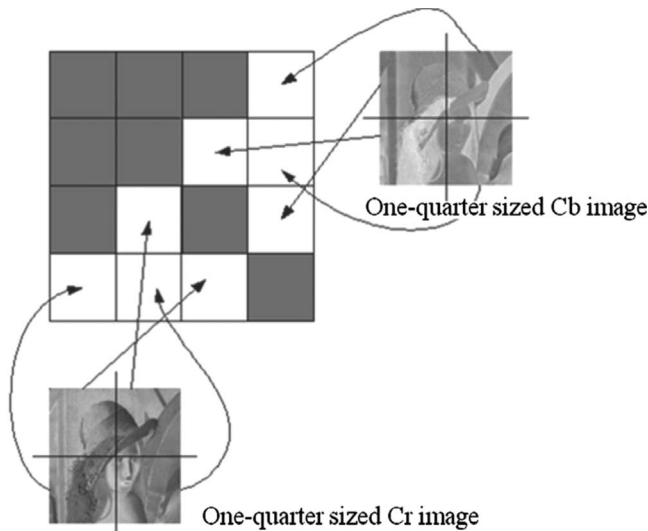


Figure 6. Method of embedding one-quarter sized CbCr components using eight subbands.

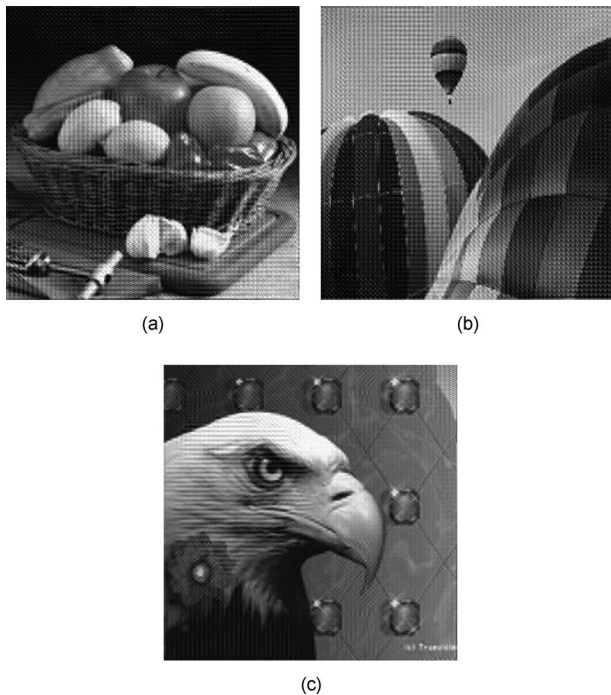


Figure 7. Textured gray images using eight subbands for embedding CbCr components: (a) fruit image; (b) balloon image; and (c) eagle image.

eight subbands is shown in Figure 6, where the quarter-sized CbCr images are divided into four regions of the same size instead of down sampling to one-sixteenth of the size CbCr images. Each separate region of the Cb image is then embedded into the DH, HH, HV, and HD subbands. Meanwhile, each separate region of the Cr image is embedded into the DV, VH, VV, and VD subbands, respectively. Next, an inverse wavelet transform is applied to obtain a textured gray image.

Figure 7 shows the textured gray images when using all eight subbands to embed the CbCr components. Here, since each separate CbCr image forms independent patterns, this

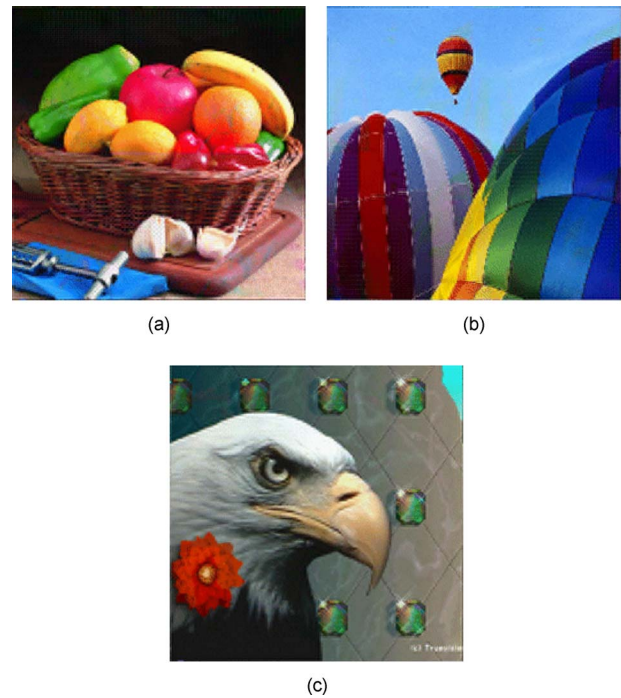


Figure 8. Recovered color images using the textured gray images in Fig. 7: (a) fruit image; (b) balloon image; and (c) eagle image.

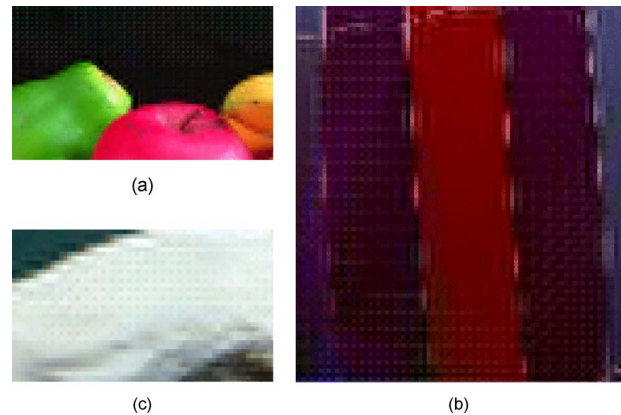


Figure 9. Partially enlarged images in Fig. 8: (a) fruit image; (b) balloon image; and (c) eagle image.

generates many visible artifacts via the inverse wavelet packet transform. These patterns also affect the recovered color images, as shown in Figure 8 and the partially enlarged images in Figure 9, where artifacts appear around the apple and pepper in the fruit image, around the violet region in the balloon image, and around the head region in the eagle image.

Table II compares the color difference and PSNR value when using eight subbands and two subbands to embed the CbCr components, confirming a better performance when using only two subbands.

Embedding a Pseudorandom Code for Compensation of Saturation

When a textured gray image is printed and scanned, the pixel values (eight bits: 0–255) of the textured gray image are

Table II. Comparison of the color difference and the PSNR value when eight subbands and two subbands were used for embedding the CbCr components.

	Fruit		Balloon		Eagle	
	Color difference	PSNR	Color difference	PSNR	Color difference	PSNR
Using eight subbands for embedding CbCr	7.41	24.25	6.53	25.61	3.98	29.75
Using two subbands for embedding CbCr	5.73	27.90	4.67	27.86	3.93	31.12

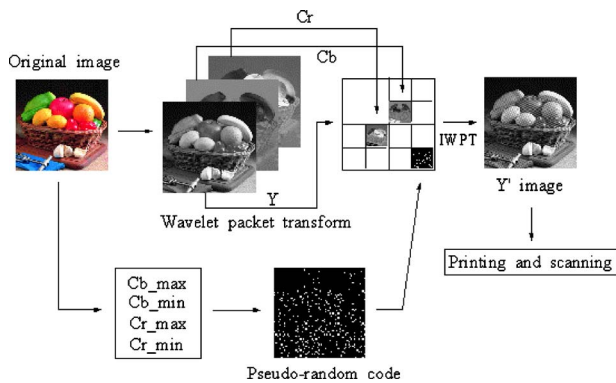


Figure 10. Process of the color-to-gray algorithm.

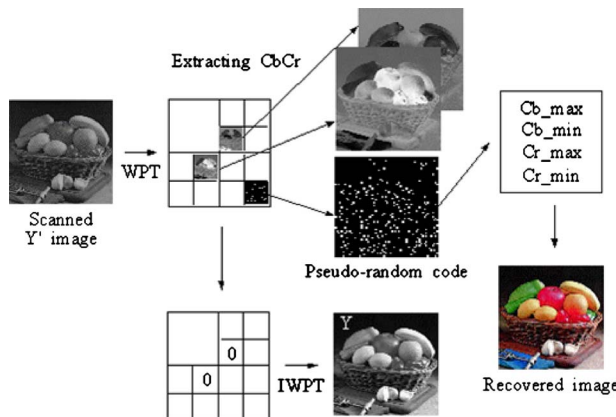


Figure 11. Process of the gray-to-color algorithm.

invariably changed by the inherent characteristics of the printer and scanner. This effect leads to a loss of color saturation in the recovered color image as the values of the embedded CbCr components are also changed in the printing and scanning process. Thus, to enhance the color saturation of the recovered color image, the CbCr components were scaled using the maximum and minimum values of the CbCr components of the original image. The processes of the proposed color-to-gray and gray-to-color algorithms are shown in Figures 10 and 11, respectively. When using the ratio of the original CbCr values to the extracted CbCr values, the color saturation of the recovered color image can be enhanced. Therefore, this information is transformed into a pseudorandom code, considering the visibility of the textured patterns in the new gray image, and then embedded into the DD subband. Consequently, these values can be

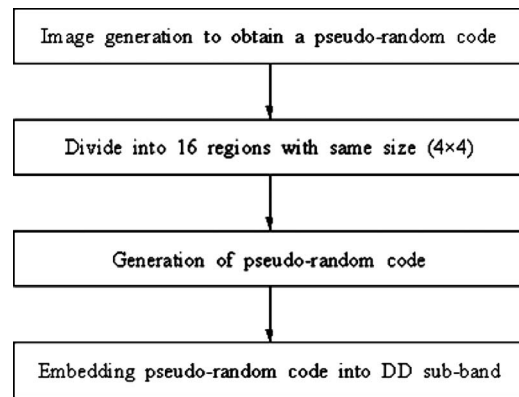


Figure 12. Flowchart for generating a pseudorandom code.

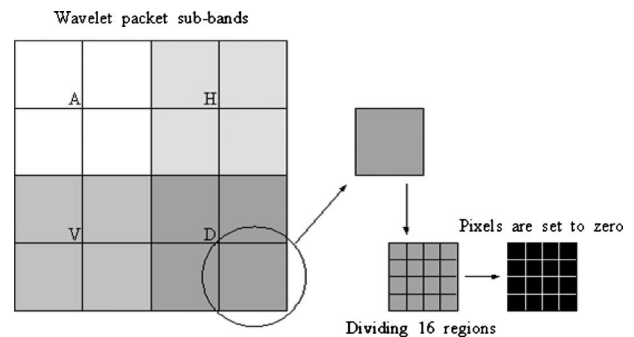


Figure 13. Image generation for embedding a pseudorandom code.

extracted in the gray-to-color process and used to compensate for the color saturation in the recovered color image.

Generation of Pseudorandom Code

The pseudorandom code is expressed by the number of white pixels according to a given code book, and the location of each pixel is chosen pseudorandomly. The procedure used to generate the pseudorandom code is shown in Figure 12. First, an image is generated that is the same size as each wavelet packet subband. This image is then divided into 16 regions with 4×4 blocks of the same size, and the subband pixel values are set to zero, as shown in Figure 13. Next, the pseudorandom code is generated using the maximum and minimum values of the CbCr components, as shown in Figure 14. Although the range of CbCr values is generally -128 – $+127$, the range may be changed to -64 – $+63$ to allow more effective representation of the CbCr information by the pseudorandom code. Next, the tens digit is separated

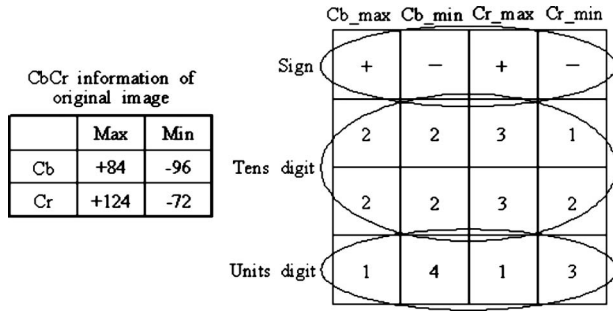


Figure 14. Example of embedding the maximum and minimum values of the CbCr components of an original image.

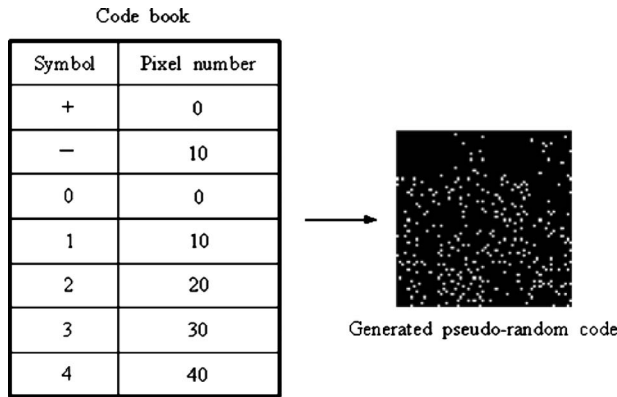


Figure 15. Code book for pseudorandom code and generated pseudo-random code using Figure 14.

into two parts, while the units digit is divided by a factor of 2. As a result, the first row of the pseudorandom code represents the sign information, the second and third rows represent the tens digit information, and the last row represents the units digit information. Meanwhile, the first and second columns of the pseudorandom code are the maximum and minimum Cb values, respectively, while the third and last columns are the maximum and minimum Cr values, respectively. For example, the maximum Cr value (+124) is represented by the pseudorandom code in Fig. 14. First, +124 is reduced to +62. Next, the tens digit (6) is separated into two parts: 3 and 3; i.e., the tens digit (6) is represented by the sum of 3 and 3. Finally, the units digit (2) is reduced by half. The maximum and minimum values for the CbCr components of the original image are then embedded into the generated image using numbers of white pixels based on a code book. Figure 15 shows the code book and pseudorandom code generated using Fig. 14.

Embedding and Extracting Method of Pseudorandom Code

The maximum and minimum values of the CbCr components of the original image are embedded into the DD subband and transformed into a pseudorandom code while considering the visibility in the new gray image. The embedding method is as follows.

When the pixel value of the location (i, j) is zero in the pseudorandom code, the pixel value is not changed if the difference between the pixel value of the location (i, j) and

the average value of the adjacent pixels in the DD subband is less than a given threshold T . However, the pixel value is changed to the average value if the difference between the pixel value of the location (i, j) and the average value of the adjacent pixels in the DD subband is more than the given threshold T .

Meanwhile, if the pixel value of the location (i, j) is not zero in the pseudorandom code, the pixel value is not changed providing the difference between the pixel value of the location (i, j) and the average value of the adjacent pixels in the DD subband is more than a given threshold T . However, the pixel value is changed to the sum of the average value and the threshold value T if the difference between the pixel value of the location (i, j) and the average value of the adjacent pixels in the DD subband is less than the given threshold T . This procedure prevents the appearance of visible patterns in the new gray image.

Compensation of CbCr Values in the Recovered Color Image

To compensate for the loss of color saturation, scaled CbCr components are used in the gray-to-color process. That is, the color saturation of the recovered color image is enhanced using the ratio of the original CbCr values to the extracted CbCr values. Since the absolute values of the CbCr extracted in the gray-to-color process are generally smaller than the absolute values of the CbCr from the original image,³ the loss of color saturation can be lessened by scaling the values of the extracted CbCr components as follows:

$$\begin{cases} \text{Cb}_{comp} = \alpha_1 \times \text{Cb} \\ \text{Cr}_{comp} = \beta_1 \times \text{Cr} \end{cases} \quad \text{for positive values of Cb and Cr,} \quad (3)$$

$$\begin{cases} \text{Cb}_{comp} = \alpha_2 \times \text{Cb} \\ \text{Cr}_{comp} = \beta_2 \times \text{Cr} \end{cases} \quad \text{for negative values of Cb and Cr,} \quad (4)$$

$$\alpha_1 = \left\lfloor \frac{\text{Cb}_{\max,o}}{\text{Cb}_{\max,e}} \right\rfloor, \quad \beta_1 = \left\lfloor \frac{\text{Cr}_{\max,o}}{\text{Cr}_{\max,e}} \right\rfloor, \quad (5)$$

$$\alpha_2 = \left\lfloor \frac{\text{Cb}_{\min,o}}{\text{Cb}_{\min,e}} \right\rfloor, \quad \beta_2 = \left\lfloor \frac{\text{Cr}_{\min,o}}{\text{Cr}_{\min,e}} \right\rfloor, \quad (6)$$

where Cb_{comp} and Cr_{comp} denote the compensated CbCr values, α and β are the scaling factors for the positive and negative values of the CbCr components, respectively, $\text{Cb}_{\max,o}$ and $\text{Cr}_{\max,o}$ denote the maximum CbCr values from the original image, $\text{Cb}_{\min,o}$ and $\text{Cr}_{\min,o}$ denote the minimum CbCr values from the original image, $\text{Cb}_{\max,e}$ and $\text{Cr}_{\max,e}$ are the maximum CbCr values extracted from the gray image, and $\text{Cb}_{\min,e}$ and $\text{Cr}_{\min,e}$ are the minimum CbCr values extracted from the gray image.



Figure 16. Test images: (a) fruit and (b) eagle.

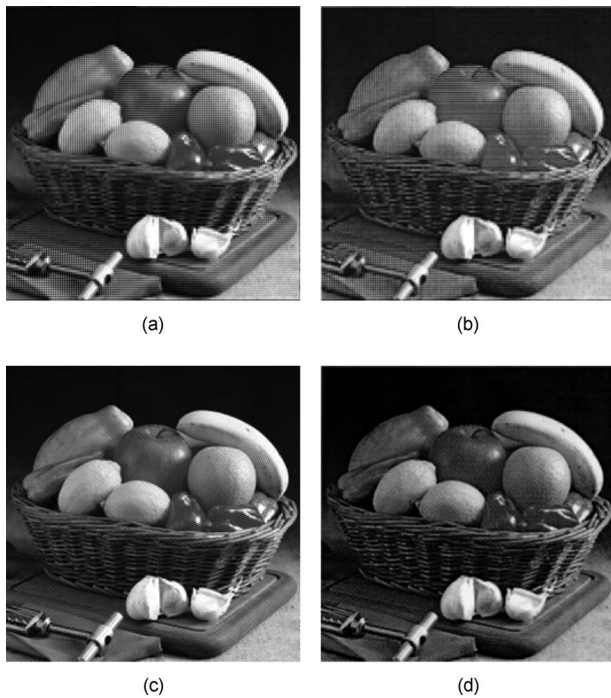


Figure 17. Comparison of the printed and scanned Y' image (fruit): (a) Y' image using the conventional method; (b) scanned image of (a); (c) Y' image using the proposed method; and (d) scanned image of (c).

EXPERIMENTAL RESULTS AND DISCUSSION

In the experiments, the method of Braun and de Queiroz was used to allow the proposed method to be compared with the best conventional method. The conventional method was more robust as regard to decoding opposite colors caused by a small image shift as the chrominance information is divided into four planes, $Cr+$, $Cr-$, $Cb+$, and $Cb-$, which are then embedded into the vertical, diagonal, horizontal, and diagonal of the approximated subbands, respectively.^{6,7} The test images used to analyze the performance of the proposed method are shown in Figure 16. The HP LaserJet 2200DN printer and the Epson Perfection V700 scanner were also used to compare the performance of the conventional method and the proposed method.

Figures 17 and 18 show the textured gray images and the printed and scanned images. Figs. 17(a) and 18(a) show the textured gray images using the conventional method and Figs. 17(b) and 18(b) show the printed and scanned images

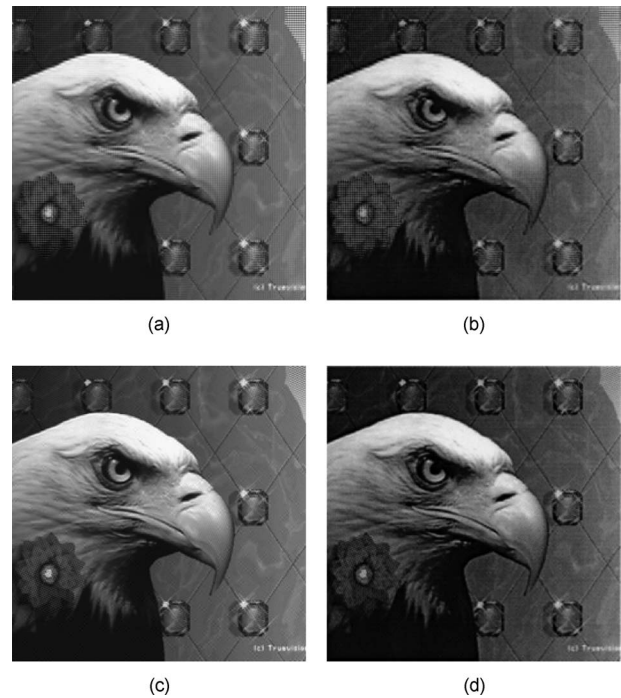


Figure 18. Comparison of the printed and scanned Y' image (eagle): (a) Y' image using the conventional method; (b) scanned image of (a); (c) Y' image using the proposed method; and (d) scanned image of (c).

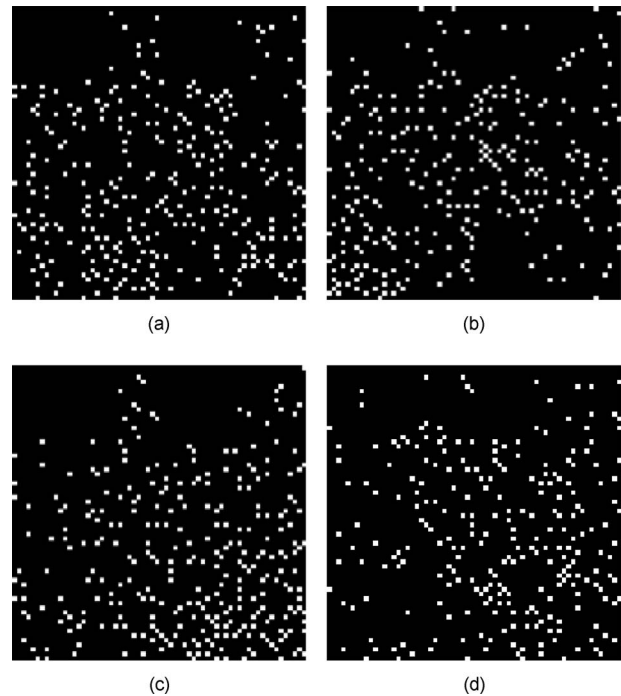
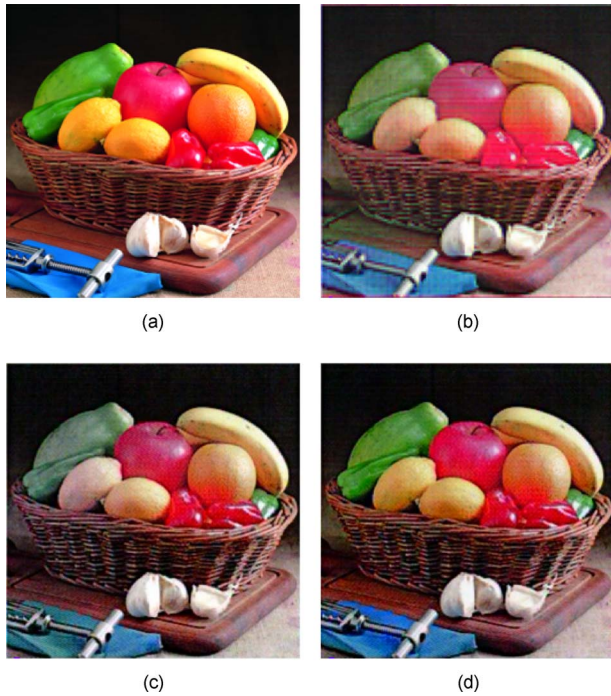


Figure 19. Comparison of original pseudorandom code and recovered pseudorandom code: (a) original pseudorandom code of fruit; (b) recovered pseudorandom code of fruit; (c) original pseudorandom code of eagle; and (d) recovered pseudorandom code of eagle.

in Fig. 17(a) and 18(a), respectively. Similarly, Figs. 17(c) and 18(c) show the textured gray images using the proposed method with the two-level wavelet packet transform and Figs. 17(d) and 18(d) show the printed and scanned images corresponding to Figs. 17(c) and 18(c), respectively. In the

Table III. CbCr errors of recovered pseudorandom codes.

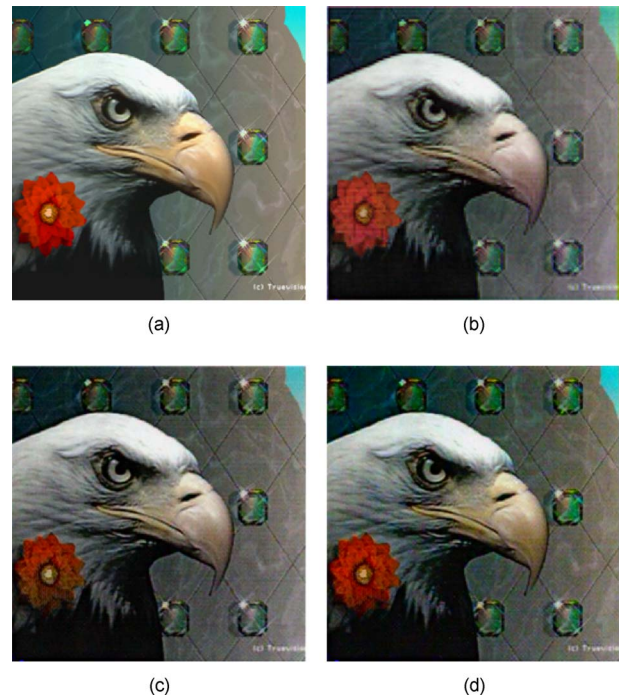
	Fruit		Eagle	
	Original	Recovered	Original	Recovered
Cb_{max}	+84	+92	+48	+46
Cb_{min}	-96	-88	-88	-84
Cr_{max}	+124	+120	+96	+92
Cr_{min}	-72	-64	-116	-108

**Figure 20.** Comparison of the recovered color image (fruit): (a) the original image; (b) the conventional method; (c) the proposed method without a compensation algorithm; and (d) the proposed method with a compensation algorithm.

conventional method, four subbands (vertical, horizontal, diagonal, and diagonal of approximation) are used to embed the Cb and Cr components. Therefore, the textures that are changed according to the Cb and Cr components appear as visible patterns in the new gray image. On the other hand, textures are less visible in the proposed method. This is because we used only two subbands (horizontal subband of the vertical subband and vertical subband of the horizontal subband) to embed the Cb and Cr components, and the area that is used for embedding color components is much smaller than that of the conventional method.

Figure 19 shows a comparison of the original pseudorandom codes and recovered pseudorandom codes. Figs. 19(a) and 19(c) show the original pseudorandom codes for the fruit and eagle images, respectively, while Figs. 19(b) and 19(d) show the recovered pseudorandom codes after the printing and scanning process. The given threshold values, T , were 35 and 32.

Table III compares the difference in the maximum and

**Figure 21.** Comparison of the recovered color image (eagle): (a) the original image; (b) the conventional method; (c) the proposed method without a compensation algorithm; and (d) the proposed method with a compensation algorithm.**Table IV.** Comparison of color difference and PSNR for recovered color images.

	Fruit		Eagle	
	ΔE_{ab}^*	PSNR	ΔE_{ab}^*	PSNR
Conventional method	20.61	18.41	18.03	18.31
Without compensation	20.28	18.73	16.79	18.79
With compensation (proposed method)	14.93	20.89	13.57	20.18

minimum values of the CbCr information between the original and recovered pseudorandom codes, where the errors between original and recovered CbCr values were less than 8, demonstrating that the proposed pseudorandom code method for compensating the CbCr values was effective for improving the color saturation of the printed and scanned gray image.

Figures 20 and 21 show a comparison of the recovered color images for fruit and eagle, respectively. Figs. 20(a) and 21(a) show original images and Figs. 20(b) and 21(b) show the recovered color images using the conventional colorization method based on the wavelet transform. Figs. 20(c) and 21(c) show the recovered color images using the proposed method without the CbCr compensating algorithm, while Figs. 20(d) and 21(d) show the recovered color images using the proposed colorization method with the CbCr compensating algorithm based on the pseudorandom code method.

Finally, Table IV shows the performance of the proposed colorization method according to the color difference and PSNR values, where the color differences were enhanced

by 5.68 and 4.46, respectively, and the PSNR values were enhanced by 2.48 and 1.87 dB, respectively.

Consequently, the proposed colorization method was shown to improve the color saturation of the recovered color images.

CONCLUSIONS

This article has proposed a color-to-gray and recovery method based on embedding a pseudorandom code in a wavelet packet transform, thereby reducing the degradation of saturation and preserving the details from the original image. First, to reduce the loss of details in the recovered color image, the CbCr color components are embedded into the two subbands with the minimum amount of energy in the Y image. Next, to compensate the color saturation in recovered color image, the CbCr components are scaled using the maximum and minimum values of the CbCr components from the original image. This information is then embedded into the DD subband using a pseudorandom code while considering the visibility in the new gray image. In other words, the pseudorandom code includes the maximum and minimum values of the CbCr components from the original image and is expressed using numbers of white pixels. However, the number of pixels is down sampled to preserve the original information in the diagonal-diagonal subband. In the reverse process, saturation of the recovered image is compensated by applying the ratio of the original CbCr values to the extracted CbCr values. In experiments, the performance of the proposed pseudorandom code method was analyzed using color difference and PSNR values, and the results confirmed that the proposed pseudoran-

dom code method improved the color saturation in the recovered color images.

ACKNOWLEDGMENTS

This work was supported by Midcareer Researcher Program through NRF grant funded by the MEST (Grant No. 2010-0000401)

REFERENCES

- ¹V. Tsagaris and V. Anastassopoulos, "Fusion of visible and infrared imagery for night color vision", *Displays* **26**, 191–196 (2005).
- ²M. Vilaseca, J. Pujol, and M. Arjona, "Color visualization system for near-infrared multispectral images", *J. Imaging Sci. Technol.* **49**, 246–255 (2005).
- ³T. Chen, Y. Wang, V. Schillings, and C. Meinel, "Grayscale image matting and colorization", *Proceedings of the ACCV2004* (Springer, Jeju, 2004), pp. 1164–1169.
- ⁴T. Welsh, M. Ashikhmin, and K. Mueller, "Transferring color to grayscale images", *Proceedings of the ACM SIGGRAPH* (ACM, San Antonio, TX, 2002), pp. 277–280.
- ⁵A. Toet, "Colorizing single band intensified night vision images", *Displays* **26**, 15–21 (2005).
- ⁶K. M. Braun and R. L. de Queiroz, "Color to gray and back: Color embedding into textured gray images", *Proc. IS&T/SID 13th Color Imaging Conference*, (IS&T, Springfield, VA, 2005), pp. 120–124.
- ⁷R. L. de Queiroz and K. M. Braun, "Color to gray and back: Color embedding into textured gray images", *IEEE Trans. Image Process.* **15**, 1464–1470 (2006).
- ⁸P. Campisi, D. Kundur, D. Hatzinakos, and A. Neri, "Compressive data hiding: An unconventional approach for improved color image coding", *EURASIP J. Appl. Signal Process.* **2002**, 152–163 (2002).
- ⁹K. W. Ko, O. S. Kwon, C. H. Son, and Y. H. Ha, "Color embedding and recovery based on wavelet packet transform", *J. Imaging Sci. Technol.* **52**, 010501 (2008).
- ¹⁰M. Chaumont and W. Puech, "A color image hidden in a gray-level image", *CGIV 2006 Final Program and Proceedings* (IS&T, Springfield, VA, 2006), pp. 226–231.
- ¹¹N. Ohta and A. R. Robertson, *Colorimetry Fundamentals and Applications* (Wiley, London, 2005).